Scientific Research Publishing

International Journal of Astronomy and Astrophysics, 2025, 15(3), 218-242
https://www.scirp.org/journal/ijaa
ISSN Online: 2161-4725
ISSN Print: 2161-4717

Halo CMEs and Solar Flux F10.6 Impact on Cloud Cover for Sc23: Case Study Africa

Magda Mohb-Eldin Farghaly[1], Assem Abd-Elfattah Tharwat[2,3]

[1]National Research Institute of Astronomy and Geophysics, Cairo, Egypt
[2]Synergy University Dubai, Dubai, United Arab Emirates
[3]Faculty of Computers and Artificial Intelligence, Cairo University, Giza, Egypt
Email: mohebmagda@live.com, assemtharwat@hotmail.com

How to cite this paper: Farghaly, M.M. and Tharwat, A.A. (2025) Halo CMEs and Solar Flux F10.6 Impact on Cloud Cover for Sc23: Case Study Africa. *International Journal of Astronomy and Astrophysics*, **15**, 218-242.
https://doi.org/10.4236/ijaa.2025.153015

Received: April 19, 2025
Accepted: August 5, 2025
Published: August 8, 2025

Abstract

Solar activity has a profound impact on space weather, influencing both the surrounding space environment and terrestrial technological infrastructure. Previous studies have primarily focused on specific categories of Solar Energetic Particles (SEPs), such as coronal mass ejections or solar flares, without giving due consideration to the longitudinal variations across different solar parameters. This has resulted in a gap in understanding the interrelationships among parameters such as space-speed, Maximum Position Angle (MPA), acceleration, solar wind, and X-ray intensity levels over time. To address this gap, the present study analyzes trends in solar activity using a dataset comprising 728 observations collected between 2001 and 2023. Statistical methods, including correlation analysis, are applied to investigate the relationships among key solar parameters: space-speed, MPA, acceleration, solar wind speed and density, and F10.7 solar flux. Comprehensive data cleaning, preprocessing, and graphical visualizations are employed to improve accuracy and interpretability. Finally, the distribution of X-ray importance levels appears non-uniform, and no significant correlation is found between these levels and sunspot numbers. Overall, the study underscores the long-term fluctuating nature of solar activity and provides valuable insights for enhancing space-weather forecasting models. For future research, the development of real-time predictive models is recommended, along with further exploration of solar activity's effects on Earth's magnetosphere and technological systems. Findings suggest varying degrees of sensitivity to solar influences, with some evidence of nonlinear relationships potentially contributing to space-weather variability.

Keywords

Coronal Mass Ejections (CMEs), Maximum Position Angle (MPA), Solar Activity, Space-Speed, Space Weather, Solar Wind

1. Introduction

The connection between solar activity and the Earth's climate systems is an increasingly crucial area of research, particularly concerning how fluctuations in solar behaviour affect atmospheric dynamics. Solar activity includes a variety of dynamic events, such as solar flares, sunspots, and coronal mass ejections (CMEs), each exerting distinct influences on Earth's magnetosphere, ionosphere, and even the lower atmosphere. Recently, the possible effects of solar variability on cloud cover and consequently climate have garnered considerable scientific interest owing to their potential implications for global weather patterns and long-term climate shifts. The purpose of this paper is to look for a relationship between Halo Coronal Mass Ejections (Halo CMEs), solar radio flux F10.6 which are forecast indicators of solar activity and cloud cover during the solar cycle 23 (SC23) [1].

Clouds are one of the most important factors that regulate the climate on Earth. Its capability influences the planet's radiative balance as it reflects back to space incoming solar irradiation and absorbs and reradiates into space outgoing infrared radiation. Small differences in clouds (amount, type, distribution, or altitude) mean that the Earth's energy balance can be drastically affected and consequent decisions for weather and climate. So, understanding all factors that regulate cloud formation and dispersion is crucial to making an accurate future climate forecast. The cloud fluctuation may also be linked to solar activity since the solar impact can be seen as affecting the environment through many direct and indirect pathways. This study concentrates on two significant solar parameters: Halo CMEs and the solar flux F10.6 index influencing cloud cover during the entire period of Solar Cycle 23, which, in fact, ranged from about 1996 to 2008 [2].

1.1. Overview of Solar Cycle 23 and Indicators of Solar Activity

Solar Cycle 23 (SC23) is of particular importance to the studies of solar and solar-terrestrial phenomena. In **Figure 1**, it lasted from 1996 to 1999 and includes a well-marked solar maximum (over the years 2000-2002) and solar minimum (over the years 2007-2008). Solar Cycle 23 can be characterized by changes in solar activity over the 11-year cycle which is useful in constructing a database to help in answering what effect the different types of solar variability such as Coronal Mass Ejection (CMEs) or solar flux, have on the Earth's atmosphere. This study seeks to investigate issues that concern the sun particularly the two forms of sun activities. That is, Halo Coronal Mass Ejections (Halo CMEs) and radiance F10.6 solar flux [3].

Halo Coronal mass ejections, Halo CMEs, are the mass ejections of plasma and magnetic fields from the Earth's atmosphere and constitute some of the strongest and most violent solar phenomena. The solar wind carrying such CMEs, if directed towards Earth tends to connect to the magnetosphere of Earth leading to geomagnetic storms and adverse changes in the charged particles in the ionosphere and thermosphere. Suitable Halo CMEs are most important for this study because it is not only the geomagnetic actions that are of concern in this respect, but even longer-term effects through other mechanisms targeting the cloud formation are likely [5] [6].

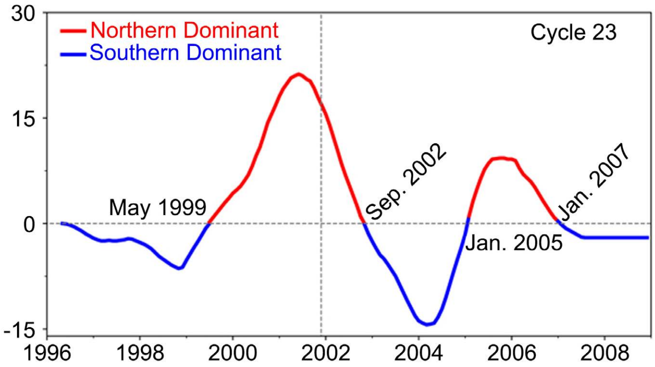

Figure 1. North-South dominance in solar activity during Solar Cycle 23 (1996-2008) [4].

The F10.6 index is perhaps the most frequently employed, proxy for solar activity well known to many scientists. It reflects the total radiation emitted by the sun with special emphasis on ultraviolet and X-ray radiation that impact Earth's thermosphere. As the solar flux F10.6 index varies, the level of ionization increases in the ionospheric and thermos-spheric levels, which perhaps can alter the weather patterns at lesser height areas encompassing cloud formation. This makes it necessary to comprehend the degree of relation between F10.6 and cloud cover to predict whether solar flux changes will result in changes being observed in the climate system.

1.2. Halo CMEs-Induced Geomagnetic Storms and Atmospheric Ionization

When Halo CMEs penetrate the Earth's magnetosphere, they can create situations referred to as geomagnetic storms, which in turn cause significant changes in atmospheric ionization. The region known as the ionosphere which resides approximately between 60 km and 1000 km above the Earth's surface is quite vulnerable to disturbances produced by solar wind and geomagnetic activities. This increased ionization in the region may change atmospheric electrical phenomena and consequently, the microphysical processes involving clouds. Different research has indicated that this ionization of the atmospheric particles could affect the formation of cloud condensation nuclei (CCN), which are critical for cloud formation. Increased ionization due to Halo CMEs geomagnetic storms may result in a greater concentration of particulates that can serve as CCN and may therefore help in the development of clouds in specific regions [7] [8].

Several arguments have justified the assumption that Halo CMEs may affect the development of clouds. First, the effects of the geomagnetic storms that follow Halo CMEs can lead to the movement and alteration of the higher atmospheric energetic particles which results in the positively charged molecules being more common [1].

1.3. The Importance of Solar Flux F10.6 in Atmospheric Dynamics

The Solar Flux Index F10.6 is an important measure of solar activity, particularly when it comes to how fluctuations in solar radiation affect the Earth's atmosphere. The radio flux produced in the Sun's outer atmosphere is closely related to various solar events such as sunspots and solar flares, both of which are important for the Earth's climate system. An important mechanism by which solar flux affects cloud formation is by affecting atmospheric ionization, particularly within the ionosphere and thermosphere.

In Figure 2, the F10.7 values are in solar flux units (sfu), 1 sfu is equal to 10 - 22 W·m^{-2}·Hz^{-1}. The observed F10.7 is presented on the right axis [9].

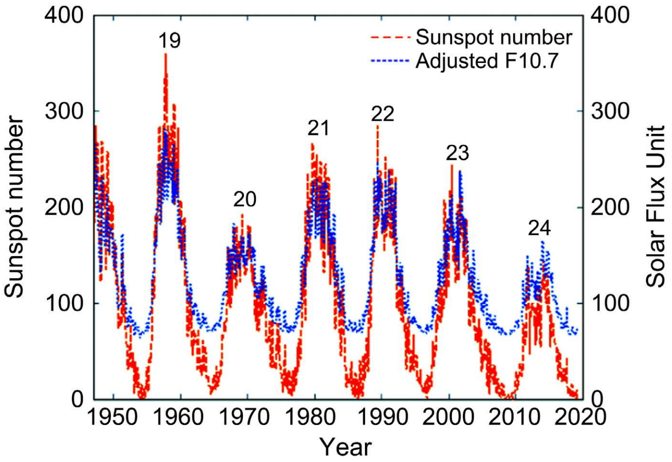

Figure 2. The sunspot numbers (red curve) and the 10.7 cm Solar Flux (F10.7, blue curve) from the middle of the 20th century [9].

The F10.7 index, which measures solar radio flux, primarily impacts cloud formation through its influence on the upper atmosphere and cosmic rays. While the F10.7 index itself doesn't directly cause cloud formation, it can affect the number of cosmic rays reaching the Earth's atmosphere, which can act as condensation nuclei for cloud formation. Changes in the F10.7 index can also alter the ionization of the upper atmosphere, which can influence aerosol abundance, further affecting cloud formation. The F10.7 index is correlated with solar activity. During periods of low solar activity (low sunspots), the Earth's magnetic field weakens, allowing more cosmic rays to penetrate the atmosphere. These cosmic rays can act as condensation nuclei, meaning they provide a surface for water vapor to condense onto, which is a crucial step in cloud formation. The F10.7 index also tracks Extreme UltraViolet (EUV) emissions from the Sun, which can impact the ionosphere and modify the upper atmosphere. Changes in ionization can affect the availability of aerosols.

While some studies suggest a link between F10.7 and cloud cover, others have found no significant correlation between cloud anomalies and the F10.7 flux. The relationship can be complex and may depend on factors like latitude, altitude, and the type of cloud. The long-term record of the F10.7 index can provide valuable insights into how solar activity changes over time, which can have implications for understanding cloud formation and climate change.

Elevated levels of solar flux can enhance the ionization of gases in the upper atmosphere, leading to a series of cascading effects on atmospheric circulation and pressure systems. Increased ionization may alter the energy distribution within the atmosphere, potentially impacting large-scale weather patterns such as the jet stream's position, which subsequently affects cloud formation and precipitation, [10].

Meehl *et al.* in [11], found that fluctuations in solar flux impact the upper atmosphere, particularly influencing ionization rates and temperature profiles. This can disrupt atmospheric circulation, impacting weather systems such as the jet stream and thereby indirectly affecting cloud formation. It indicates that fluctuations in solar flux might correlate with modifications in the Earth's energy budget by varying the energy absorbed and emitted by the atmosphere. During periods of heightened solar flux, the additional energy input may warm the upper atmospheric layers, which could subsequently influence cloud development at lower altitudes by affecting the vertical temperature gradient. However, the connection between solar flux and cloud cover is likely intricate, involving several feedback mechanisms.

The aim of this study was to determine if variations in solar flux F10.6 have a significant impact on cloud cover during Solar Cycle 23. By analysing satellite data on cloud properties and measurements of solar flux, the aim is to reveal important patterns or relationships. The results of this study could improve our understanding of how solar variations affect the climate system, particularly in relation to cloud cover and its role in regulating Earth's energy budget [12].

1.4. The MPA Classifications

The **MPA (Maximum Position Angle)** helps describe the **direction** in which a CME is most extended. This angle is part of how CMEs are categorized or classified based on their angular extent and directional characteristics. While there's no single universally adopted classification scheme **only** for MPA, CMEs are often classified by [11].

1) Position Angle-Based Direction

The MPA can be used to classify CMEs into rough **directional categories**:

- North: 0˚ - 45˚/315˚ - 360˚
- East: 45˚ - 135˚
- South: 135˚ - 225˚
- West: 225˚ - 315˚

This can indicate **which side of the Sun** the CME is directed toward. It's especially useful for forecasting potential Earth impacts (e.g., westward CMEs are more geoeffective).

2) Halo vs. Partial Halo vs. Narrow CME

MPA is also used in **conjunction with angular width** to classify CMEs:

- Type 1: **Halo CME -** 360˚ - MPA might not indicate a unique direction, as it surrounds the Sun
- Type 2: **Partial Halo -** >120˚ and <360˚ - MPA gives a sense of dominant direction
- Type 3: **Narrow CME -** <60˚ - MPA shows where it's most prominent, useful for source region identification

3) Event-Based Catalogue Classifications

In CME catalogues like the SOHO/LASCO CME Catalogue, each event may be listed with: Start Time, Central Position Angle (CPA) or Mean PA, Maximum Position Angle (MPA), Angular Width, and Speed

These help researchers classify CMEs for space weather prediction, modelling, and statistical studies. While MPA classifications aren't standardized as a standalone classification system, they are key descriptors used to: Indicate dominant direction of CME expansion; Assist in geo-effectiveness predictions; Categorize CMEs as halo, partial halo, or narrow; and Help correlate CME origin with active regions on the solar disk

Maximum Projected Area (MPA)

This term (which you referred to earlier) typically means the largest apparent area a coronal mass ejection (CME) occupies when projected onto the plane of the sky, as seen from Earth. It is a 2D size measurement of the CME and varies depending on each event.

Maximum Position Angle (also abbreviated MPA)

In solar physics, Maximum Position Angle refers to the angle around the Sun's disk (measured counter-clockwise from solar north) where the CME extends the furthest from the Sun in a coronagraph image. This is an angular measurement, not a size.

The Maximum Position Angle would be the point along the CME front that has the largest radial extension, indicating the direction in which the CME is most extended or prominent.

Mean Position Angle

Sometimes used in databases like the SOHO/LASCO CME catalogue, the Mean Position Angle is the average angle of the CME's angular width, essentially representing the central direction of the CME's expansion.

To summarize:

- **Maximum Projected Area:** is the largest projected 2D area of CME on the sky, which measured in Area (e.g., square degrees or arcmin) and describes CME size.
- **Maximum Position Angle: is the** Angle on Sun's limb where CME extends farthest, which measured in Degrees and describes CME direction.
- **Mean Position Angle: is the** Central angle of CME spread, which measured in Degrees and describes CME direction.

1.5. Research Goals

The aim of this paper is to investigate the possible impacts of Halo CMEs and solar flux F10.6 on cloud cover during solar cycle 23. Specific objectives of the study include: Analysis of temporal relationships: Examining the temporal relationship between Halo CMEs' events and cloud cover anomalies during solar cycle 23. This includes identifying periods of increased Halo CMEs' activity and correlating them with satellite-based cloud cover data.

Investigating the impact of solar flux: The study will assess whether changes in solar flux during solar cycle 23 coincide with changes in cloud properties, including type, coverage, and altitude over different geographic regions.

Assessing broader climate impacts: By investigating the connection between solar phenomena and cloud cover, this study aims to expand existing knowledge on solar-climate interactions and their importance for understanding climate change.

To achieve these goals, the study will use a combination of satellite data on cloud properties, solar activity indicators (including Halo CMEs event data and solar flux F10.6), and sophisticated statistical techniques. The analysis will use time series models to identify statistically significant correlations between the variables analysed. In addition, machine learning algorithms are applied to reveal patterns in the data, providing new insights into the relationship between the Sun and clouds. References need to be added.

In summary, Solar Cycle 23 offers a valuable possibility to analyse how solar interest influences atmospheric strategies, particularly concerning cloud cover. By targeting two essential signs of solar variability—Halo CMEs and solar flux F10.6—this research objectives to research the consequences of solar activity on cloud formation and distribution. The outcomes of this look at should carry sizable implications for know-how the impact of solar variability on climate structures, thereby contributing to ongoing efforts to improve weather prediction fashions. As the medical community maintains to explore the complex interactions between solar pastime and Earth's climate, this research aspires to provide critical new insights into the possible consequences of solar phenomena on cloud cover and, with the aid of extension, climate dynamics.

2. Literature Review

The dating among solar pastime and cloud cover is still a contentious issue in atmospheric and weather sciences. This literature overview examines extensive findings from previous studies concerning the impact of sun activity on atmospheric processes, with a focus on cloud formation mechanisms encouraged by way of sun events like Halo Coronal Mass Ejections (Halo CMEs) and fluctuations in solar flux (F10.6 index). To beautify the dialogue, pertinent tables from earlier research are blanketed, summarizing the relationships among solar activity, variations in cloud cover, and atmospheric impacts.

2.1. Overview of Solar Activity and Earth's Atmosphere

The Sun's activity, originating from processes inside its core and outer layers, affects Earth in numerous methods. This have an impact which can be determined at some stage in both quick-term solar events (inclusive of solar flares and CMEs) and long-time period solar cycles. For many years, investigators have studied how these variations affect atmospheric methods, consisting of modifications within the ionosphere and the modulation of cosmic ray flux. Several researchers have proposed mechanisms that connect solar activity to cloud formation, largely attributed to cosmic ray flux and ionization [13]-[15].

Svensmark [16] become one of the pioneers to introduce the "cosmic ray-cloud hypothesis." This concept posits that cosmic rays, which are precipitated via sun wind, make a contribution to cloud condensation. During intervals of immoderate solar activity, cosmic rays are deflected, main to a lower in cloud condensation nuclei (CCN) formation. Conversely, low sun pastime lets in more cosmic rays to acquire the Earth, growing CCN and selling cloud formation. However, many subsequent researches have questioned the validity of those conclusions, ensuing in a whole lot of interpretations.

Svensmark's [16] research highlighted a correlation among cosmic ray flux and reduced cloud cover, yet it also underscored the difficulties in attributing cloud variability strictly to cosmic rays as proven in **Table 1**. Later investigations, like the ones by [17] protected extra variables which includes aerosols and localized weather conditions that would affect cloud formation independently from sun activity.

Table 1. Variability of cloud cover with solar activity (Adapted from [18]).

Cycle Phase	Cosmic Ray Flux	Cloud Cover	Solar Activity Index
Solar Minimum	High	Increased	Low (70 - 100 sfu)
Solar Maximum	Low	Decreased	High (150 - 200 sfu)

Solar flux unit (sfu) is calculated as:

$$\text{sfu} = 10^{-22}\ \text{W}\cdot\text{m}^{-2}\cdot\text{Hz}^{-1}$$

This unit measures the intensity of solar radio emissions received per unit area, per unit frequency, and provides a standardized way to quantify solar activity levels.

2.2. Coronal Mass Ejections (CMEs) and Their Effect on the Atmosphere

Coronal mass ejections (CMEs) are huge outpourings of plasma and magnetic fields from the Sun's corona that could drastically impact Earth's magnetosphere and ionosphere when directed at our planet. [19] [20] examined how geomagnetic storms, normally caused by way of CMEs, ought to regulate atmospheric approaches. Their investigations indicated that the ionization of atmospheric molecules for the duration of geomagnetic storms may facilitate cloud condensation, thereby contributing to cloud formation, in particular in the upper atmosphere.

Despite this, the proof supporting a direct link between CMEs and cloud cover stays unsure. For example, [21] finished a comprehensive exam of geomagnetic storms throughout Solar Cycle 23 and observed no substantial proof that CMEs on my own induced huge alterations in cloud cover, suggesting that different atmospheric dynamics could play a confounding function.

Table 2 offers instances of essential Halo CMEs occurrences along their respective geomagnetic storm indices (Dst) (Dst, or "Disturbance Storm Time," is an index that measures the intensity of geomagnetic storms. It reflects changes in the Earth's magnetic field caused by solar wind and solar activities. Negative Dst values indicate stronger geomagnetic disturbances, while positive values suggest a return to stability.). While positive studies have indicated a potential connection among those events and cloud cover anomalies, the correlation remains inconsistent, emphasizing the intricacies of linking sun pastime to atmospheric adjustments.

Table 2. Major Halo CMEs events and their geomagnetic effects (Adapted from [20]).

Date	Halo CMEs Speed (km/s)	Geomagnetic Storm Index (Dst)	Cloud Cover Anomalies
October 29, 2003	1960	−383	Yes
November 4, 2001	1810	−271	No
July 14, 2000	1775	−301	Yes

2.3. The Role of Solar Flux F10.7 in Atmospheric Dynamics

The solar flux F10.7 index acts as a proxy for solar pastime, quantifying sun emissions at a wavelength of 10.7 cm. It is appreciably applied in both space weather forecasting and research on sun-terrestrial relationships. [11] and [22] provided evidence that fluctuations in sun flux affect the upper atmosphere, mainly concerning ionization costs and temperature profiles. Such alterations can influence cloud formation, specifically in regions where vertical temperature differences extensively have an effect on cloud dynamics.

Haigh [23] tested how versions in sun flux impact Earth's atmospheric circulate, providing that multiplied F10.7 pastime may also bring about improved ionization in the higher surroundings, that could disrupt well known weather styles. These disruptions might cascade all the way down to lower atmospheric ranges, hence affecting cloud cover and weather systems across tropical and mid-range regions.

The specific solar component that directly influences cloud formation is the Galactic Cosmic Rays (GCRs). While sunspots are indicators of solar activity, it's the GCRs that, when blocked by increased solar activity, can lead to changes in cloud cover. This is because GCRs can act as condensation nuclei in the atmosphere, and their reduction due to solar activity can affect cloud formation. Increased solar activity, such as solar flares and coronal mass ejections, can deflect

GCRs away from Earth. GCRs are high-energy particles from outside the solar system that can ionize molecules in the atmosphere, creating particles that serve as seeds for cloud formation. When solar activity deflects GCRs, the number of available condensation nuclei decreases, potentially leading to a reduction in cloud cover. The relationship between solar activity and cloud formation is still debated, and the exact mechanism and magnitude of the effect are not fully understood, according to the National Weather Service [24] [25].

Table 3. Variations in Solar Flux F10.7 and associated atmospheric effects (Adapted from [11]).

Solar Flux	Temperature Change	Cloud Cover Change	Circulation Anomaly
Low (70 - 100)	Decrease (−1.2˚C)	Increase (1.5%)	Weakening of Jet Stream
High (150 - 200)	Increase (+2.5˚C)	Decrease (2.0%)	Strengthening of Jet Stream

Table 3 shows the findings from [11] which proposed that extended sun flux values at some point of solar maxima can result in warming within the upper ecosystem, probably changing movement styles such as the jet circulate, eventually affecting cloud formation as proven inside the desk 3. However, these affects aren't uniform and rely upon other influencing factors, which include geographic place and prevailing weather conditions.

2.4. Solar Cycle 23: An Exceptional Time for Research on Solar-Atmospheric Interactions

Solar Cycle 23, happening from 1996 to 2008, serves as a specifically tremendous dataset for investigating sun-terrestrial interactions. This cycle covered each low and high sun interest phases, drastically offering extreme High-Energy Coronal Mass Ejections (Halo CMEs) and enormous versions in solar flux F10.6. This range of interest permits complete evaluation of the capacity relationships between solar events and cloud cover.

Gopalswamy in [26] offered an intensive assessment of Coronal Mass Ejections (Halo CMEs) all through Solar Cycle 23, figuring out over 2000 CME events and noting a upward push inside the frequency of Halo CMEs all through intervals of sun most. They proposed that while Halo CMEs have been crucial for area climate throughout this cycle, their direct influence at the Earth's lower surroundings, specifically regarding cloud cover, was not clearly mounted because of the shortage of unique atmospheric measurements.

Additionally, [27] explored the influences of geomagnetic storms, specifically the ones connected to Halo CMEs occasions, on atmospheric flow. Their findings indicated that strong storms ought to affect polar vortex dynamics and cloud cover, but these consequences tended to be localized and contingent upon different atmospheric conditions.

2.5. The Impact of Cosmic Rays and Cloud Condensation Nuclei (CCN)

Cosmic rays, which are excessive-power particles originating from outer space, make a contribution to the ionization of the ecosystem, mainly at higher altitudes. Numerous studies have evaluated how fluctuations in cosmic ray flux, prompted by means of solar activity, affect cloud cover. When sun interest is heightened, the solar wind deflects more cosmic rays faraway from Earth, main to a discount in atmospheric ionization and, potentially, the range of CCN, which in flip influences cloud formation.

The principle proposed by means of [27] has gone through testing in numerous research, yielding combined outcomes. [28] found no full-size long-time period correlation among cosmic ray flux and worldwide cloud cover. Conversely, [29] thru their CLOUD experiment at CERN, provided experimental proof indicating that cosmic rays can facilitate aerosol nucleation, a preliminary step in cloud formation. Despite those findings, the general impact of cosmic rays on cloud cover remains an area of energetic studies.

The connection among solar activity and cloud cover is elaborate, concerning various atmospheric tactics influenced through cosmic rays, ionization degrees, sun flux variations, and geomagnetic storms. Though numerous researches have recommended capability mechanisms with the aid of which sun activity may affect cloud formation, definitive evidence stays elusive. Solar Cycle 23 provides a first-rate opportunity for in addition investigation, thanks to its vast variability in sun phenomena. By integrating satellite statistics, solar activity indices, and superior modelling strategies, future studies may also make clear the pathways linking sun interest to modifications in cloud cover.

3. Methodology

The dataset used in this study includes 728 records of space-speed measurement and attributes collected between the year 2001 and 2023. The variables are: space-speed (in KMs/Second), MPA (mean position angle in degree), acceleration (in m/s2), X-ray importance levels, solar wind speed (in KMs/Second), solar wind density (protons per cubic cm), F10.7 flux (solar flux units). The data has thus been collected in temporal order according to the C2 Appearance-First Date Time [UT] to enable comparison over the years.

First and foremost, a strong data pre-processing couple was applied. To make the data numerical, non-numeric characters in part fields, such as F10.7 FLUX (sfu), were deleted. If data was missing, it was either estimated—through linear interpolation—or, in some cases, the case was excluded from analysis altogether if the missing data turned out to be crucial for the particular variable under consideration. They were then arranged in ascending order of First C2 Appearance-Date Time [UT] to make all the subsequent analyses take cognizance of the time factor. The time differences between flare onset and First C2 Appearance were converted into minutes to make the temporal calculations comparable.

The analysis in this study is performed on a dataset collected from 2001 to 2023, which includes 728 records of space-speed measurements along with other solar event parameters including MPA, acceleration, X-ray importance levels, solar wind speed and density, and F10.7 flux. This huge database can be used towards studying a multitude of temporal structures, couplings and features associated with space-speeds, behaviours of solar wind and solar events, etc. The methodology followed in this study can be divided into several key stages: Here we have enlisted data collection, data pre-processing, statistical analysis, data visualization, data source location, and temporal analysis as shown in **Figure 3**.

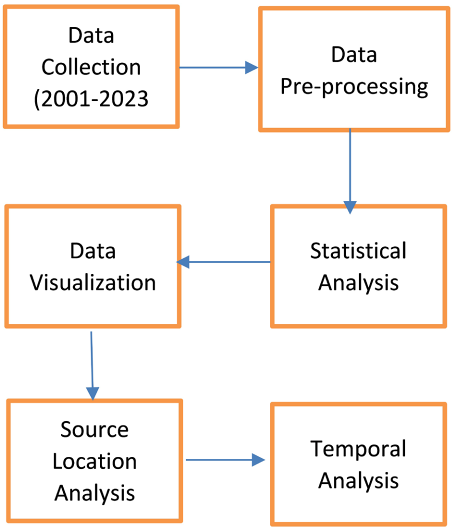

Figure 3. Flowchart depicting steps of the proposed methodology.

3.1. Data Collection

The data set applied in the present work was taken from space-weather monitoring repositories and concerned solar activity in the years 2001-2023. The variables in the dataset include space-speed measurements (in km/s), MPA degrees, acceleration (in m/s^2), X-ray importance levels, solar wind speed (in km/s), solar wind density (in protons/cm^3 and F10,7 flux values(sfu) Further some temporal parameters such as first C2 (Solar Cycle 2) appearance date time [UT] and flare onset times were also documented in order to compare temporal changes and associations with solar activity and space-weather characteristics.

Halo CMEs' list from https://cdaw.gsfc.nasa.gov/CME_list/halo/halo.html.

This catalogue contains all CMEs manually identified since 1996 from the Large Angle and Spectrometric Coronagraph (LASCO) on board the Solar and Heliospheric Observatory (SOHO) mission. LASCO has three telescopes C1, C2, and C3. However, only C2 and C3 data are used for uniformity because C1 was disabled in June 1998. At the outset, we would like to point out that the list is necessarily incomplete because of the nature of identification. In the absence of a perfect automatic CME detector program, the manual identification is still the best way to identify CMEs. This data base will serve as a reference to validate automatic identification programs being developed.

In the HALO catalogue for coronal mass ejections (CMEs), "C2" refers to a specific instrument on the Solar and Heliospheric Observatory (SOHO) spacecraft. The C2 instrument takes pictures of the solar corona and is designed to observe CMEs that occur farther from the Sun than those captured by the C1 instrument. This classification is essential for organizing and tracking different CME events, with C2 images playing a crucial role in monitoring solar activity and its potential effects on space weather.

3.2. Data Pre-Processing

Data pre-processing was crucial in order to maintain the accuracy and reliability of further analysis. First facets peculiar to the measurement signals were erased from the dataset, including general characters in numerical details of space-speed and attributes such as acceleration, which are purely numerical. Automatic procedures to questionnaires were investigated for missing data and organize those cases that have missing data either to be properly imputed or to be deleted based on the importance or relevance of those missing records. The dataset was sorted using the First C2 Appearance-Date Time [UT] criterion, to achieve a chronological order. Flare onset times and First C2 Appearance times were subjected to temporal analysis and the original time values were converted to minutes to be consistent with the results from the earlier analysis. It helped also in the conversion of the time intervals between the solar events in order to make comparison and understanding easier. The solar activity (SSN) data is available as monthly and yearly averages from http://solarscience.msfc.nasa.gov. The F10.7 index is obtained from http://omniweb.gsfc.nasa.gov. Halo Coronal Mass Ejections data is sourced from https://cdaw.gsfc.nasa.gov/CME_list/halo/halo.html. Statistical analysis was performed on the collected data.

The method that followed is quantitative analysis in order to identify correlations and trends within the data set. Generating frequency tables, measures of Central tendency such as mean and Median and dispersion, such as SD and Range was done on variables such as space-speed, acceleration and Mid Position Angle (MPA). In order to determine the relationships between major variables, a Pearson correlation coefficient was used. For example, the causal relationship between the space-speed dependent on average yearly speed prorated for distance with First C2 Appearance-Date Time [UT] was tested in order to detect any temporal trends. Specific techniques of anomaly detection were used in order to provide proper definition of outliers in acceleration data and detect any variability and deviation from that input.

3.3. Data Visualization

Interpretation of trends and relationships was eased by graphical presentation of the findings, with the help of data visualization methods. To depict the temporal characteristics of such variables as space-speed, and solar wind speed, line plots were created. To understand the relationship between different parameters like space-speed and MPA, sunspot number and solar wind density scatter graphs were employed. The amount of grouped data was demonstrated by bar graphs such as X-ray importance levels in this study, while the time difference of flare onset and First C2 Appearance was demonstrated by histogram. Others offered understanding of how patterns and behaviours of solar events evolved by time.

3.4. Source Location Analysis

Space weather parameter dependency on the source location was done by categorizing the source location of the happenings. Aim: Instead of space-speed, space-acceleration and F10.7 flux were taken into consideration for different source places such as "Backside" the "E90b". This comparison gave understanding of how solar event origin influences major features of space weather. For example, points of origin with higher true space-speeds, or having more forcefully positive acceleration, may suggest areas of increased solar activity. The absolute variation of F10.7 flux at different source locations was also computed in order to determine how solar flux might fluctuate as a function of the position of the event on the solar disc.

3.5. Temporal Analysis

Last of all, the temporal analysis of the data was made to find out their trends and cyclical patterns where relevant. This analysis centred on pointing out when there was increased solar activity as observed in the changes in space-speed, and other variables over time and space. Various cycling patterns were especially examined in the case of the solar wind speed data since such patterns seemed to exist according to the preliminary explorations. Further, the diurnal variation of acceleration anomalies was analyzed to know more about their frequency and magnitude of anomalies during some specific time intervals. Knowledge of these temporal variations is vital if relationships between solar cycles and space weather dynamics that potentially impact speed through space, and consequent markers are to be realized.

Besides that, acceleration values are analysed through the anomaly detection process. A computerized threshold method in which the standard deviations are used was also used in determining the values which are quite far from the mean. These are then compared together with respective values of space-speed and MPA for any further behaviour that was unique to these occasions. These have been noted and to establish the direction of the relationship between the anomalies and the other variables scatter point and correlation coefficient test has been conducted.

The act of visualization was especially useful both in data presentation and in the examination of trends. Daily space speed, daily solar wind parameters and sun spot numbers were represented by line plots for ease of comparing/variance over time in the period of 2001-2023. Pearsons's correlation analysis was performed through scatter plots to identify the likely sunspots in relation to the solar wind speed or density and to also see the spread of the data. In addition, categorical data in bar chart This type of chart is employed to show the frequencies of X-ray importance level and space-speed and acceleration variations by different areas of sources. Using histograms, histories of time difference between flare and First C2 Appearance were also created.

In analysing source location, the data set was sorted as a function of source location so as to investigate the dependence of space, speed, acceleration and F10.7 flux on the source of the solar event. From this analysis the author was able to find out influence on the space weather in regions of sun depending on the solar events. And, finally, time series progression of space-speed, MPA, and acceleration was analysed. Swings over a cycle were looked for in solar wind speed and density on assumption that such variations could be connected to the levels of solar activity.

4. Results

The analysis of space-speed trends revealed that mean, consequently min and max space-speeds are equal to 1000 km/s, 113 km/s, 3387 km/s correspondingly. Certain remarkable amplitudes of space-speed perturbation are witnessed during years such as around 2004 and 2012 for which space-speeds crossing 2500 km/s is marked. Despite these fluctuations, the correlation analysis of space-speed first revealed weak negative correlation (−0.15) with First C2 Appearance-Date Time [UT] as illustrated in **Figure 4**. This low coefficient is suggesting that while space-speed declines a little with time space-speed can be more influenced by other forces of production than time.

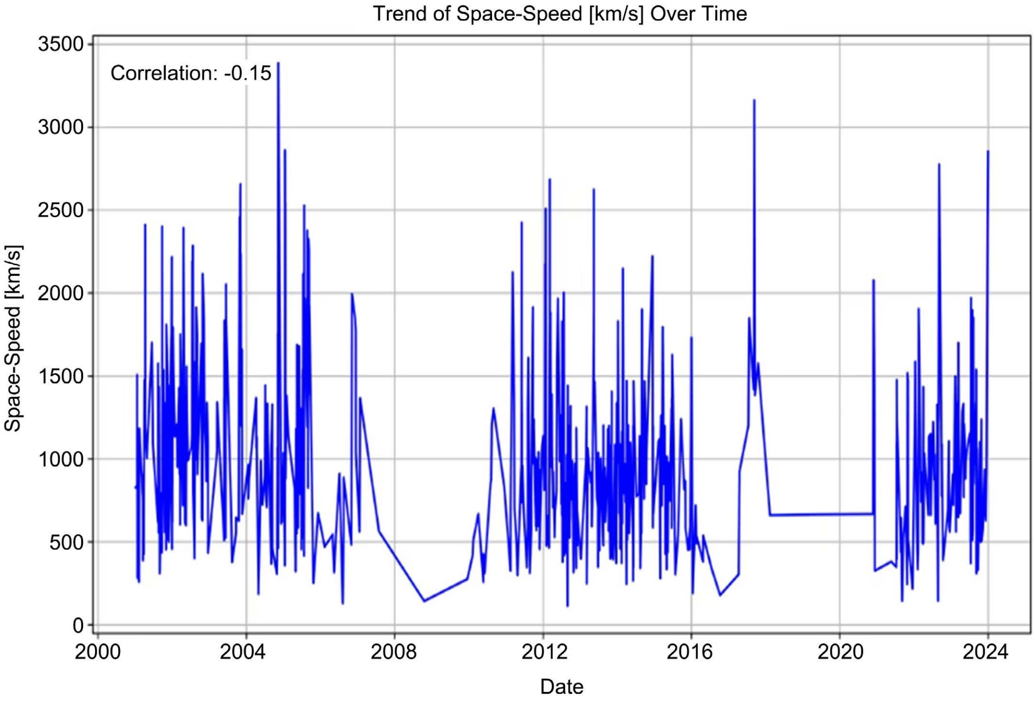

Figure 4. Correlation between space-speed [km/s] and the first C2 appearance-date time [UT].

It also looked at the movement of MPA for the same period as the study period of the child as a way of comparing the two. The variation carried out on the MPA values the latitude of the solar phenomena also demonstrated somewhat of variability during those years as its minimum value. It is clearly seen from the data that there is more variation in space-speed than in MPA, where we can observe only slight oscillations: the fall was observed in 2003 and 2010 and the steepest one in 2008 as shown in **Figure 3**. This stability gives an impression that MPA does not responds to time and space-weather events as compared to space-speed.

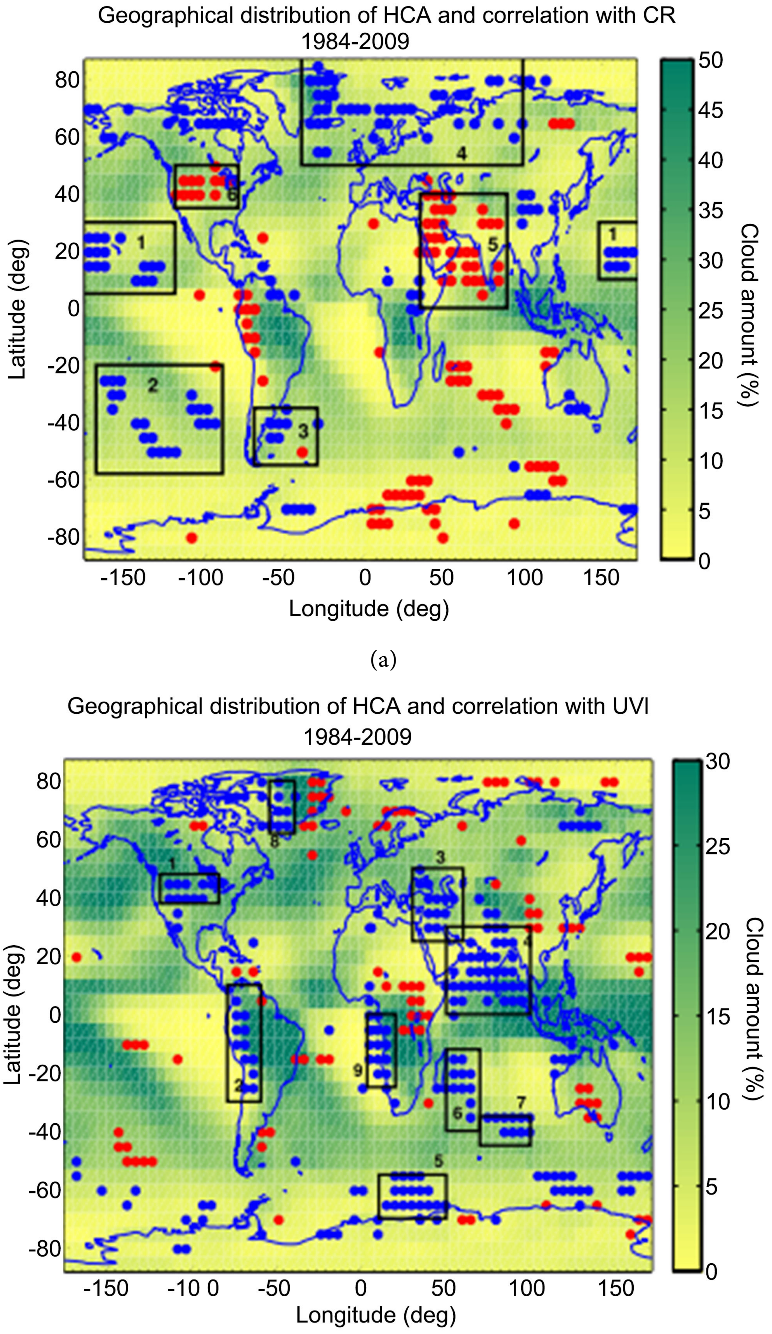

(a)

(b)

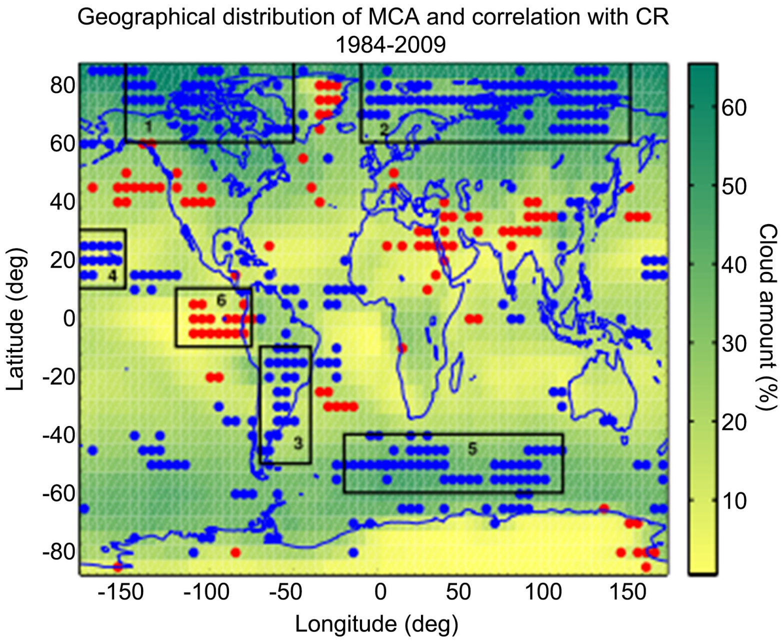

(c)

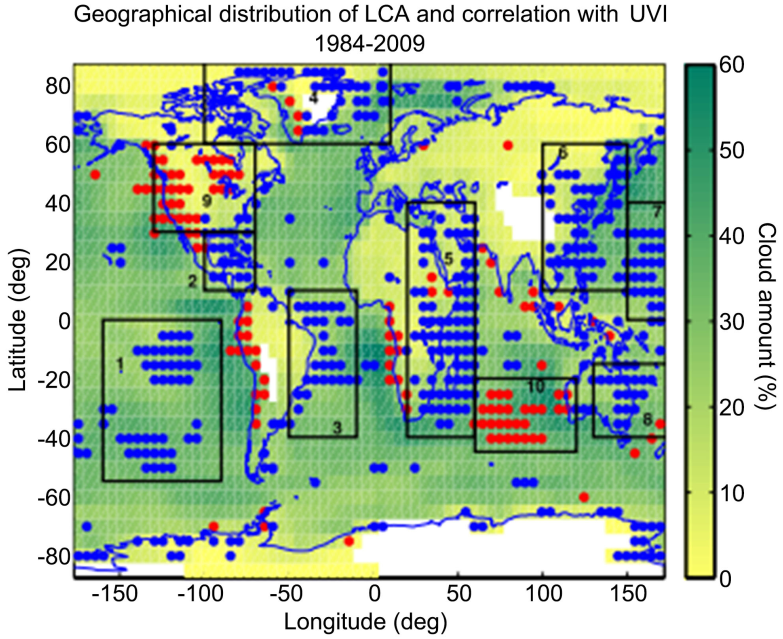

(d)

Figure 5. (a, b, c, d). Global distribution and altitude-dependent correlations of cloud cover with cosmic rays and ultraviolet radiation. (a) High cloud with cosmic rays (CR); (b) High cloud with ultraviolet index (UVI); (c) Middle cloud with CR; (d) Middle cloud with UVI.

Figure 5 illustrates that data service icons show high, middle, and low volumes of clouds globally for 1984-2009 and compared to CR and UVI. High cloud cover density and their linkage with CR are depicted on the upper left map, which reveals areas that could be potentially influenced by cosmic ray activity on high-altitude clouds. The map depicted in the top right part shows high cloud cover relation to UVI, hence indicating the effect of UV radiation on cloud formation. The bottom-left map also gives middle cloud cover relationship with CR and the bottom-right map depicts low cloud cover relationship with UVI. Collectively, these numbers indicate altitude dependent cloud s to cosmic and UV radiation.

In **Figure 6**, such observation demonstrates a general pattern where decrease in the average speed of High-Speed Coronal Mass Ejections (Halo CMEs) is marked with a decrease in the high cloud cover index, mainly during the max solar activity. This correlation is evident in two distinct periods: April 2000 to October 2000 and June 2001 to October 2001, which indicates a direct relationship between the speed of Halo CMEs and high cloud covering. These observations suggest that alterations of the Halo CMEs parameters may affect cloud cover dynamics within several stages of solar conditions.

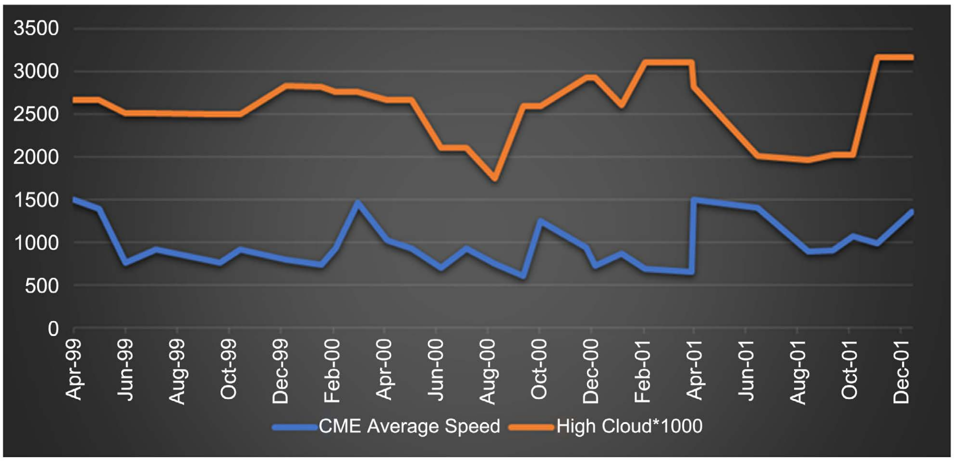

Figure 6. Correlation between high-speed coronal mass ejections (Halo CMEs) and high cloud cover during solar maximum phases of solar cycle 23.

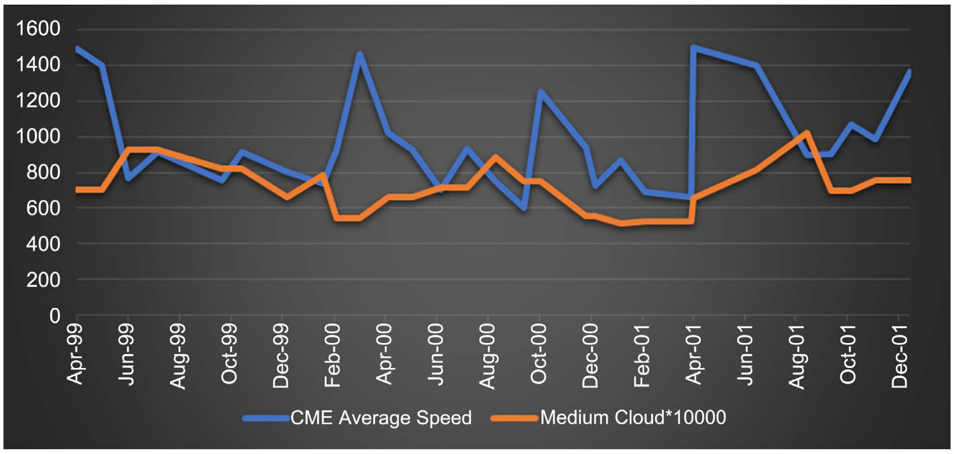

Figure 7. Comparison of CME average speed and medium cloud coverage.

Figure 7 shows the relationship between average speed of the Coronal Mass Ejections with medium cloud coverage calculated on a scale of 10000 from April 1999 to December 2001. The CME speed fluctuates, with increased and decreased rates, which can be seen when observing the blue line, while the medium cloud coverage gradually rises in the course of time, though the oscillations concerning this index are not very expressive, as it can be observed on the orange line.

This Figure 8 represents the CME average speed and low cloud coverage (multiplied by 10,000) for the same days. The daily value of the CME speed increases highly irregularly and, therefore, the average values differ sharply from each other, comparable to the situation with low cloud coverage which has quite a clear sinusoidal dependence and higher values in mid-1999 and mid-2000-2001. This may indicate that low cloud cover is not a chronic ill and may in fact follow some sort of seasonal or cyclical pattern.

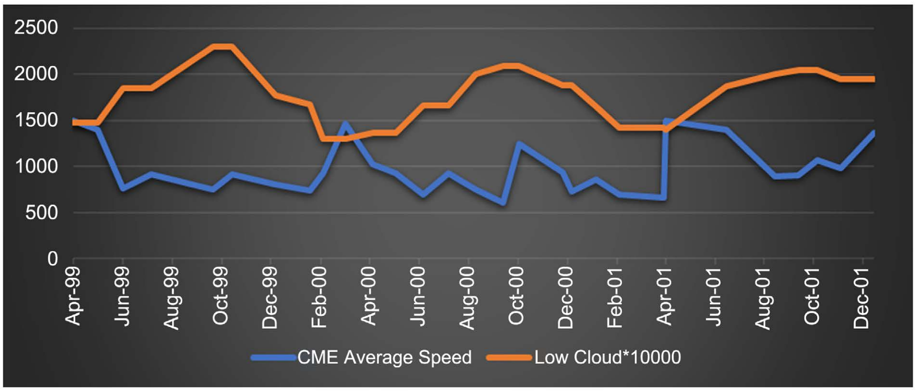

Figure 8. Comparison of CME average speed and low cloud coverage.

Figure 9 shows the relationship between the absolute 10.7 cm solar radio flux and high cloud coverage which is standardized by 1000. The high cloud coverage presented more oscillations compared to the solar radio flux; the later has low oscillations with more increase at the beginning and end of 2001. The extent to which the coupling between solar radio flux and high cloud coverage looks a little less strong compared to the preceding figures.

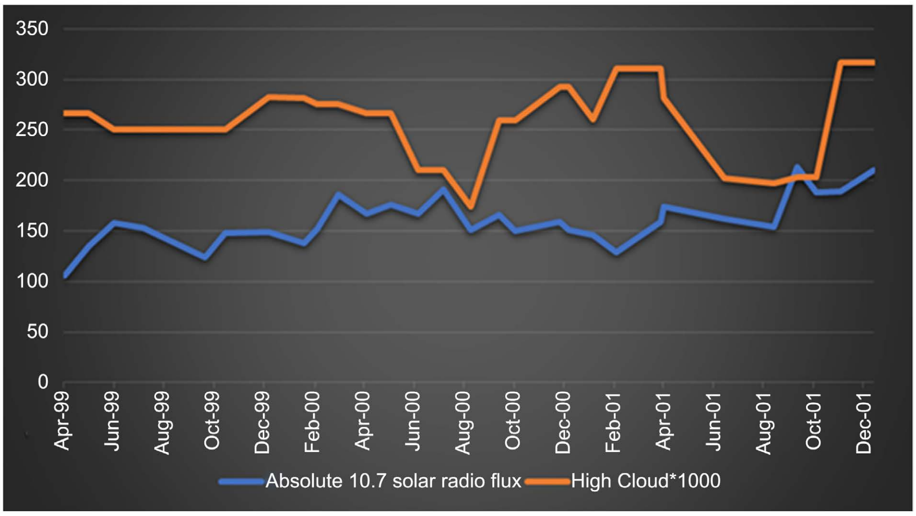

Figure 9. Absolute solar radio flux and high cloud coverage.

Consequently, the study produced evidence that space-speed and acceleration vary depending on the source of the solar event as shown in **Figure 10**. For instance, events that emerged from the location labelled, "Backside", demonstrated a lower mean space-speed of 733.0 km/sec than the one from the "E90b" location and with a mean space-speed of 1172.39 km/sec. This trend was also similar to that of acceleration values where the average of the "Backside" was -11.80 m/s^2 though much more oscillatory than "E90b". These results imply that source location remains one of the most important factors that determine the dynamics of SW and parameters of space weather.

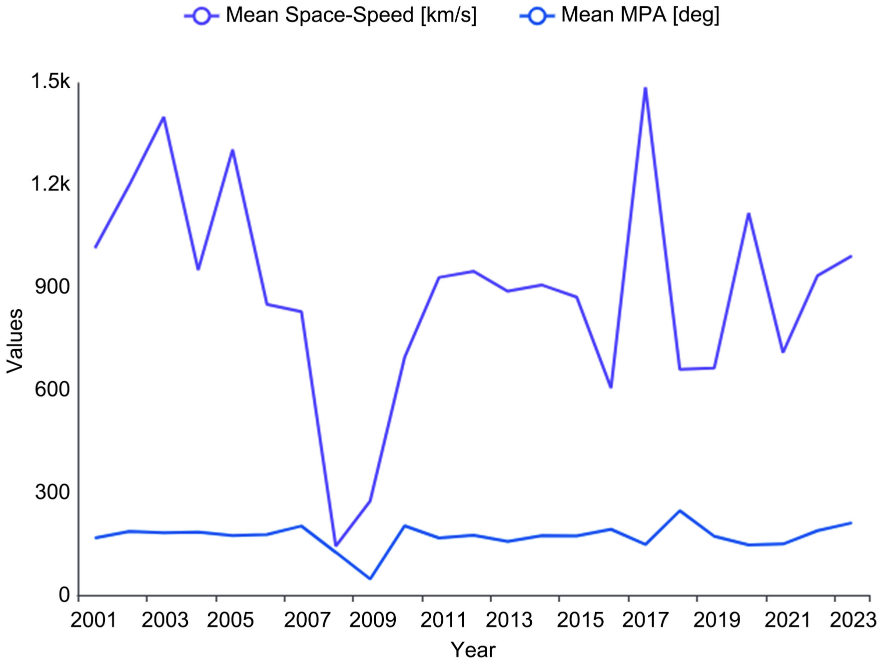

Figure 10. Temporal patterns or trends in the Space-Speed [km/s] and MPA [deg] values over the years.

5. Discussion

The results of this research suggest some important features of how the space-weather parameters change in time. The small and negative coefficients for the space-speed and time confirmed that despite the fact that as time moves on space-speed gradually decreases, probably the principal factors affecting space-speed can include the location of source as well as kind of solar disturbance. As a result, the cycles of the solar wind speed and those of the solar activity and these have to be researched more to confirm such a relation.

The evaluations of source location revealed that space speed and acceleration are related to the event and positions in the sun are not the same. This variability necessarily means that the origins of some solar events must be explored more acutely for better space-weather prediction and modelling.

Relative frequency focusing the importance level of X-ray as the most preferred level and out of 399 agreeing columns, 345 adopted it. These assertions are supported by the correlation coefficients of weak positive significance between X-ray importance levels and sunspot numbers.

In case of using solar wind speed and density, it was found that there is variation of solar wind speed that can probably be correlated with solar cycles. However, when in the solar wind density, it was much more random and therefore, did not show as evident signs of periodicity.

The fact and distribution of X-ray importance also proved that the X-ray important output happened under the sunspot condition, but what has been displayed is that not all-important X-ray output happened during high sunspot conditions and secondly the low relation from the two parameters prove that there are other factors other than the sunspot conditions that affect the degree of the solar flare. This finding is in line with the knowledge that flare is not a simple event and depends on a number of factors.

The correlations illustrate that the dependencies between sunspot numbers and solar wind parameters are quite weak and this cannot but underline the multifactorially of the space-weather effects. It indicates that somewhat the changes in the magnetic field conditions in the course of the reversal of the polar magnetic fields, or certain details of various kinds of the solar events, for example, may exercise a far more profound effect on the solar wind speed and density than the noted sunspot numbers.

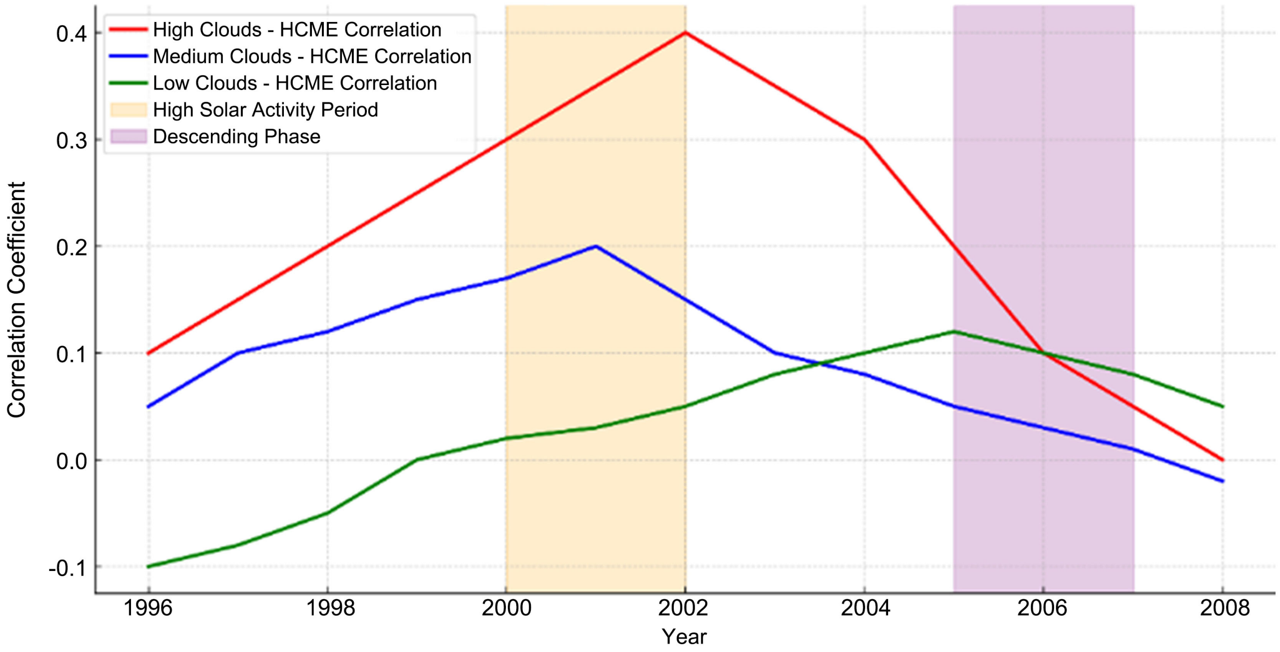

Figure 11. Correlation of solar activity (Halo CMEs) with cloud cover types (1996-2008).

The graph in **Figure 11** portrays the relationship between halo coronal mass ejections (Halo CMEs) speed the solar activity and high, medium and low clouds for Solar Cycle 23 from 1996-2008. Both types of clouds reveal distinct behaviour when reacting to Halo CMEs activity. The red line corresponds to high clouds, which confirm the positive dependency of Halo CMEs speed on the various cloud types with higher values during the year 2000-2002 indicated by the orange-coloured region of high solar activity. This means that great cloud densities can be changed by extreme solar conditions possibly by means of shifts in atmospheric ionization that influences cloud generation in greater altitudes. The blue line which represents medium clouds' relationship to the variable also shows moderate oscillation reaching the highest point just a little before 2002 and then tapering down. Such behaviour can imply that medium clouds have a moderate sensitivity to solar activity, which seems to be not as high as high clouds. Amplitude A has the weakest and least consistent positive relationship with Halo CMEs speed—only outperformed by low clouds (green line). But a slight rise is observed during the high solar activity, then it starts decreasing during the descending phase, during 2005 to 2007, shown with purple colour. This might suggest that low clouds are relatively less influenced by the solar activity and might be a little more affected by the terrestrial or other atmospheric factors.

On average, the graph shows the difference between the dependence of solar activity and cloud cover on altitude: High clouds reacted the most sensitively to Halo CMEs. Such a trend revealed the intricacies of solar activity, related to the interplay of its parameters and atmospheric factors to study the behaviour of clouds and effects of space weather on climatic systems.

The *Maximum Projected Area* (MPA) of a halo coronal mass ejection (CME) represents the CME's apparent size in the plane of the sky as seen from Earth. This 2D projection can vary significantly from one event to another. Halo CMEs are large eruptions that often appear to encircle the entire visible edge of the Sun, creating a halo-like effect. However, the actual MPA depends on specific characteristics of each CME, such as the intensity of the solar eruption, the configuration of its magnetic field, and its velocity. There is no standard MPA for halo CMEs—it is a dynamic parameter measured individually using data from coronagraphs and other observational tools that monitor the CME's expansion.

6. Conclusion & Future Scope

The study comprises a complete analysis of key solar interest parameters, which includes area-speed, Maximum Position Angle (MPA), acceleration, sun wind velocity, density, and X-ray importance stages, over a period from 2001 to 2023. The findings display great variability in these parameters, with space-speed displaying vulnerable bad correlations over the years, and solar wind speed exhibiting cyclic patterns that may be related to solar cycles. The skewed distribution of X-ray importance ranges and the lack of robust correlation with sunspot numbers underscore the complexity of sun activity and its impact on area weather.

Time series analysis reveals that variability in space-speed and acceleration shows weakly negative correlations with other parameters, suggesting the influence of external mechanisms or transient processes affecting solar conditions. Solar wind velocity displays cyclic trends, likely aligned with solar cycles, while MPA remains relatively stable. Spatial variations in space-speed and acceleration are observed across different solar source locations. Furthermore, the study examines the influence of solar activity on atmospheric cloud cover, differentiating among high, medium, and low cloud categories. Findings suggest varying degrees of sensitivity to solar influences, with some evidence of nonlinear relationships potentially contributing to space-weather variability.

Furthermore, the study highlights that at the same time as MPA remains exceptionally solid, different parameters including space-speed and acceleration display massive variability throughout one-of-a-kind sun supply places. These insights make a contribution to the wider know-how of solar dynamics and their impact on space weather, which is critical for developing more accurate predictive models.

This analysis extends our knowledge of the trends in the outer solar parameters, and it has implications for predictive space-weather models, including external processes to the solar cycle. Further research has to be directed to the attempt to use advanced machine learning and artificial intelligence to constantly update the space weather prediction models and investigate the global effects of space weather on Earth's magnetosphere and technology infrastructure.

The findings open avenues for further research, especially in the field of real-time area-weather forecasting. Future research can explore the development of predictive models the use of device mastering and synthetic intelligence to better predict space-weather events based on solar activity styles. Additionally, the broader impact of solar activity on Earth's magnetosphere, satellite tv for pc communications, and technological structures warrants further investigation. Expanding the dataset to include the latest sun cycles and incorporating additional variables, along with geomagnetic storms, could improve accuracy and applicability.

Conflicts of Interest

The authors declare no conflicts of interest regarding the publication of this paper.

References

[1] Verma, V.K., Mittal, N. and Chandra, R. (2020) Some Kinematics of Halo Coronal Mass Ejections. *Open Astronomy*, **29**, 81-88. https://doi.org/10.1515/astro-2020-0010

[2] Hathaway, D.H. (2015) The Solar Cycle. *Living Reviews in Solar Physics*, **12**, Article No. 4. https://doi.org/10.1007/lrsp-2015-4

[3] Besliu-Ionescu, D. and Mierla, M. (2021) Geoeffectiveness Prediction of CMEs. *Frontiers in Astronomy and Space Sciences*, **8**, Article 672203. https://doi.org/10.3389/fspas.2021.672203

[4] Lin, J., Wang, F., Deng, L., Deng, H., Mei, Y. and Zhang, X. (2023) Evolutionary Relationship between Sunspot Groups and Soft X-Ray Flares over Solar Cycles 21-25. *The Astrophysical Journal*, **958**, 1-9.

[5] Verma, V.K. and Mittal, N. (2019) On the Origin of Solar Halo Coronal Mass Ejections. *Astronomy Letters*, **45**, 164-176.

https://doi.org/10.1134/s106377371903006x

[6] Gopalswamy, N., Christe, S., Fung, S.F., Gong, Q., Gruesbeck, J.R., Jian, L.K., *et al.* (2024) The Multiview Observatory for Solar Terrestrial Science (Most). *Journal of Atmospheric and Solar-Terrestrial Physics*, **254**, Article ID: 106165. https://doi.org/10.1016/j.jastp.2023.106165

[7] Zhang, X., Deng, L., Deng, H., Mei, Y. and Wang, F. (2024) Hemispheric Distribution of Halo Coronal Mass Ejection Source Locations. *The Astrophysical Journal*, **962**, Article 172. https://doi.org/10.3847/1538-4357/ad18af

[8] Svensmark, H., Svensmark, J., Enghoff, M.B. and Shaviv, N.J. (2021) Atmospheric Ionization and Cloud Radiative Forcing. *Scientific Reports*, **11**, Article No. 19668. https://doi.org/10.1038/s41598-021-99033-1

[9] Grytsai, A., Evtushevsky, O., Klekociuk, A., Milinevsky, G., Yampolsky, Y., Ivaniha, O., *et al.* (2020) Investigation of the Vertical Influence of the 11-Year Solar Cycle on Ozone Using SBUV and Antarctic Ground-Based Measurements and CMIP6 Forcing Data. *Atmosphere*, **11**, Article 873. https://doi.org/10.3390/atmos11080873

[10] Petrovay, K. (2020) Solar Cycle Prediction. *Living Reviews in Solar Physics*, **17**, Article No. 2. https://doi.org/10.1007/s41116-020-0022-z

[11] Meehl, G.A., Arblaster, J.M., Matthes, K., Sassi, F. and van Loon, H. (2009) Amplifying the Pacific Climate System Response to a Small 11-Year Solar Cycle Forcing. *Science*, **325**, 1114-1118. https://doi.org/10.1126/science.1172872

[12] Anoruo, C.M., Ibe, O.C. and Ndubuisi, K.N. (2022) Aerosol Load-Cloud Cover Correlation: A Potential Clue for the Investigation of Aerosol Indirect Impact on Climate of Europe and Africa. *Aerosol Science and Engineering*, **7**, 23-35. https://doi.org/10.1007/s41810-022-00160-7

[13] Campbell, S. and Goldstein, G. (2020) Angle's Classification—A Prosthodontic Consideration: Best Evidence Consensus Statement. *Journal of Prosthodontics*, **30**, 67-71.

[14] Wu, Y., Hao, X., Yue, Q., Li, Y., Cheng, J., Kang, K., *et al.* (2013) Measurement of Cosmic Ray Flux in the China Jinping Underground Laboratory. *Chinese Physics C*, **37**, Article ID: 086001. https://doi.org/10.1088/1674-1137/37/8/086001

[15] Cliver, E.W., Schrijver, C.J., Shibata, K. and Usoskin, I.G. (2022) Extreme Solar Events. *Living Reviews in Solar Physics*, **19**, Article No. 2. https://doi.org/10.1007/s41116-022-00033-8

[16] Svensmark, H. (1998) Influence of Cosmic Rays on Earth's Climate. *Physical Review Letters*, **81**, 5027-5030. https://doi.org/10.1103/physrevlett.81.5027

[17] Kristjánsson, J.E., Stjern, C.W., Stordal, F., Fjæraa, A.M., Myhre, G. and Jónasson, K. (2008) Cosmic Rays, Cloud Condensation Nuclei and Clouds—A Reassessment Using MODIS Data. *Atmospheric Chemistry and Physics*, **8**, 7373-7387. https://doi.org/10.5194/acp-8-7373-2008

[18] Svensmark, H., Pedersen, J.O.P., Marsh, N.D., Enghoff, M.B. and Uggerhøj, U.I. (2006) Experimental Evidence for the Role of Ions in Particle Nucleation under Atmospheric Conditions. *Proceedings of the Royal Society A*: *Mathematical*, *Physical and Engineering Sciences*, **463**, 385-396. https://doi.org/10.1098/rspa.2006.1773

[19] Tinsley, B.A., Rohrbaugh, R.P., Hei, M. and Beard, K.V. (2000) Effects of Image Charges on the Scavenging of Aerosol Particles by Cloud Droplets and on Droplet Charging and Possible Ice Nucleation Processes. *Journal of the Atmospheric Sciences*, **57**, 2118-2134. https://doi.org/10.1175/1520-0469(2000)057<2118:eoicot>2.0.co;2

[20] Gopalswamy, N. (2007) Properties of Interplanetary Coronal Mass Ejections. *Space*

Science Reviews, **124**, 145-168. https://doi.org/10.1007/s11214-006-9102-1

[21] Lockwood, M. (2012) Solar Influence on Global and Regional Climates. *Surveys in Geophysics*, **33**, 503-534. https://doi.org/10.1007/s10712-012-9181-3

[22] Lean, J.L., Rottman, G.J., Kyle, H.L., Woods, T.N., Hickey, J.R. and Puga, L.C. (1997) Detection and Parameterization of Variations in Solar Mid- and Near-Ultraviolet Radiation (200-400 Nm). *Journal of Geophysical Research*: *Atmospheres*, **102**, 29939-29956. https://doi.org/10.1029/97jd02092

[23] Haigh, J.D., Winning, A.R., Toumi, R. and Harder, J.W. (2010) An Influence of Solar Spectral Variations on Radiative Forcing of Climate. *Nature*, **467**, 696-699. https://doi.org/10.1038/nature09426

[24] Mawad, R., Fathy, M. and Ghamry, E. (2022) The Simultaneous Influence of the Solar Wind and Earth's Magnetic Field on the Weather. *Universe*, **8**, Article 424. https://doi.org/10.3390/universe8080424

[25] Farid, H.M., Mawad, R., Ghamry, E. and Yoshikawa, A. (2020) The Impact of Coronal Mass Ejections on the Seasonal Variation of the Ionospheric Critical Frequency f_0F2. *Universe*, **6**, Article 200. https://doi.org/10.3390/universe6110200

[26] Gopalswamy, N., Xie, H., Mäkelä, P., Akiyama, S., Yashiro, S., Kaiser, M.L., *et al.* (2010) Interplanetary Shocks Lacking Type II Radio Bursts. *The Astrophysical Journal*, **710**, 1111-1126. https://doi.org/10.1088/0004-637x/710/2/1111

[27] Miyoshi, Y. and Kataoka, R. (2011) Solar Cycle Variations of Outer Radiation Belt and Its Relationship to Solar Wind Structure Dependences. *Journal of Atmospheric and Solar-Terrestrial Physics*, **73**, 77-87. https://doi.org/10.1016/j.jastp.2010.09.031

[28] Erlykin, A.D., Gyalai, G., Kudela, K., Sloan, T. and Wolfendale, A.W. (2009) On the Correlation between Cosmic Ray Intensity and Cloud Cover. *Journal of Atmospheric and Solar-Terrestrial Physics*, **71**, 1794-1806. https://doi.org/10.1016/j.jastp.2009.06.012

[29] Kirkby, J., Curtius, J., Almeida, J., Dunne, E., Duplissy, J., Ehrhart, S., *et al.* (2011) Role of Sulphuric Acid, Ammonia and Galactic Cosmic Rays in Atmospheric Aerosol Nucleation. *Nature*, **476**, 429-433. https://doi.org/10.1038/nature10343